Published in final edited form as:
Biofabrication. 2009 June ; 1(2): 025001. doi:10.1088/1758-5082/1/2/025001.

Hybrid biomimetic scaffold composed of electrospun polycaprolactone nanofibers and self-assembled peptide amphiphile nanofibers

Ajay Tambralli[1], **Bryan Blakeney**[1], **Joel Anderson**[1], **Meenakshi Kushwaha**[1], **Adinarayana Andukuri**[1], **Derrick Dean**[2], and **Ho-Wook Jun**[1,3]

Ho-Wook Jun: hwjun@uab.edu

[1]Department of Biomedical Engineering, University of Alabama at Birmingham, 801 Shelby Building, 1825 University Boulevard, Birmingham, AL 35294, USA

[2]Department of Materials Science and Engineering, University of Alabama at Birmingham, BEC 254, 1150 10th Ave South, Birmingham, AL 35294, USA

Abstract

Nanofibrous electrospun poly (ε-caprolactone) (ePCL) scaffolds have inherent structural advantages, but lack of bioactivity has limited their usefulness in biomedical applications. Thus, here we report the development of a hybrid, nanostructured, extracellular matrix (ECM) mimicking scaffold by a combination of ePCL nanofibers and self-assembled peptide amphiphile (PA) nanofibers. The PAs have ECM mimicking characteristics including a cell adhesive ligand (RGDS) and matrix metalloproteinase-2 (MMP-2) mediated degradable sites. TEM imaging verified successful PA self-assembly into nanofibers (diameters of 8 – 10 nm) using a solvent evaporation method. This evaporation coating method was then used to successfully coat PAs onto ePCL nanofibers (diameters of 300 – 400 nm), to develop the hybrid, bioactive scaffolds. SEM characterization showed that the PA coatings did not interfere with the porous ePCL nanofiber network. Human mesenchymal stem cells (hMSCs) were seeded onto the hybrid scaffolds to evaluate their bioactivity. Significantly greater attachment and spreading of hMSCs were observed on ePCL nanofibers coated with PA-RGDS as compared to ePCL nanofibers coated with PA-S (no cell adhesive ligand) and uncoated ePCL nanofibers. Overall, this novel strategy presents a new solution to overcome the current bioactivity challenges of electrospun scaffolds and combines the unique characteristics of ePCL nanofibers and self-assembled PA nanofibers to provide an ECM mimicking environment. This has great potential to be applied to many different electrospun scaffolds for various biomedical applications.

Keywords

Electrospinning; peptide amphiphiles; self-assembly; ECM

1. Introduction

The rationale for a tissue engineered scaffold is to repair damaged tissue by providing a biodegradable extracellular matrix (ECM) mimicking environment. The ECM is a nanofibrous network of proteins and polysaccharides, having both regulatory and structural functions. Interactions between cells and the ECM, via cell surface receptors and cell

[3] Author to whom any correspondence should be addressed.

adhesive ligands, regulate many cellular behaviors, such as adhesion, proliferation, migration, and differentiation [1 – 4]. Furthermore, nanofibrous scaffolds that mimic the topography and scale of native ECM have been shown to elicit better cellular behaviors than microfibrous scaffolds [5]. Therefore, it is essential to tailor and design tissue engineered scaffolds by mimicking the nanofibrous morphology and the biochemical complexities of native ECM. In this study, we describe the development of such a biomimetic scaffold using a combination of electrospun poly (ε-caprolactone) (ePCL) nanofibers and self-assembled peptide amphiphile (PA) nanofibers.

Electrospinning has gained a lot of attention due to its simple and cost effective method to fabricate scaffolds that can replicate the fibrillar structure of the ECM. Some advantages of electrospinning are that it has been used to produce nanofibrous scaffolds using both synthetic polymers and natural materials, and that the topographical features of the fibers can be easily adjusted to fit specific applications by controlling a number of different parameters [6]. PCL has been frequently chosen for electrospinning because it is a FDA approved, biocompatible, and biodegradable polyester. ePCL has been shown to support the attachment and growth of chondrocytes, skeletal muscle cells, smooth muscle cells, endothelial cells, fibroblasts, and human mesenchymal stem cells [5 – 13]. While these studies showed the biological efficacy of using ePCL scaffolds, their usefulness in biomedical applications is limited by their lack of bioactivity.

Several different techniques have been used to improve interactions between cells and ePCL scaffolds, such as subjecting them to plasma treatment, modifying them with ethylenediamine, co-electrospinning with poly (vinyl alcohol), and immobilizing soluble eggshell protein on their surface [10, 14 – 17]. Even though these techniques improved cell adhesion to the scaffolds, they could not improve cell-scaffold interactions to guide cell fate. To address this issue, there have also been several studies attempting to improve the bioactivity of electrospun scaffolds. Among them are electrospinning natural polymers (e.g collagen, elastin, gelatin), co-electrospinning solutions of synthetic and natural polymers (e.g. PCL/collagen, PCL/gelatin, PCL/hydroxyapatite, PCL/chitosan), and coating ePCL scaffolds with collagen, gelatin, and calcium phosphate [8 – 11, 14, 18 – 30]. While these studies demonstrated better cellular behavior on scaffolds containing the biological polymers, there are still concerns regarding immunogenicity, denaturing during fabrication, and post-production crosslinking for scaffold stability and integrity. Thus, it is imperative to develop a better strategy to endow ePCL scaffolds with bioactivity, one that ultimately provides cells with both the structural and functional characteristics of the native ECM microenvironment.

PAs consist of a hydrophilic peptide region covalently coupled to a hydrophobic alkyl tail. By changing pH or adding calcium ions, these PAs self-assemble into cylindrical micelles in a highly controlled manner to form gel-like nanomatrices [31 – 33]. The remarkable versatility of PAs, coupled with several recent design advancements, has enabled the development of a PA based nanomatrix capable of mimicking several essential properties of the ECM such as self-assembly into nanofibers, enzyme-mediated degradation, and presence of cell adhesive ligands [31].

The RGDS sequence was specifically chosen as the bioactive signal in this study, because it is a ubiquitous cell adhesive ligand found in various ECM molecules such as fibronectin, laminin, vitronectin, and collagen. It binds to several integrin receptors, such as αvβ3 and α5β1, and controls various cellular behaviors [34, 35]. Another important characteristic of the ECM is its susceptibility to enzyme-mediated degradation, which affects the rate of ECM production *in vitro* [36]. In particular, the matrix metalloproteinase (MMP) family of enzymes hydrolyzes most ECM proteins and facilitates constant matrix remodeling [1, 2,

37]. Thus, to enable intimate interactions between cells and scaffolds, the PAs in this study have been inscribed with both RGDS cell adhesive ligands and MMP-2 enzyme sensitive sites.

In this study, we demonstrated the feasibility of developing a nanostructured, ECM mimicking, hybrid scaffold with a combination of ePCL nanofibers and self-assembled PA nanofibers. It is hypothesized that the PAs can be self-assembled into nanofibrous matrices using a solvent evaporation technique onto the surface of ePCL nanofibers, thus endowing them with bioactivity. This strategy combines the distinctive characteristics of ePCL nanofibers and self-assembled PA nanofibers to provide an ECM mimicking environment. It can be applied to different electrospun polymers and used for various biomedical applications.

2. Materials and Methods

2.1. Electrospinning PCL nanofibers

PCL pellets (Sigma Aldrich, MO; M_n = 80,000) were dissolved in a solvent system of chloroform: methanol (1:1, v/v) to obtain a 22.5 wt% viscous polymer solution and collected in a syringe capped with a 25-G blunt tipped needle. The syringe was placed in a syringe pump (KD Scientific, MA) and a flow rate of 1 ml/hr was set. The needle tip was connected to a high voltage source (Gamma High-Voltage Research, FL) and a voltage of +21 kV was applied to it. The resulting electrospun PCL (ePCL) nanofibers were deposited on a grounded aluminum collector placed 28 cm from the needle tip. These were stored in a vacuum dessicator for 2-3 days to remove any residual solvents.

2.2. Peptide amphiphiles

All peptides were synthesized at a 0.30 mmol scale using standard Fmoc-chemistry in an Advanced Chemtech Apex 396 peptide synthesizer. Alkylation, cleavage, deprotection, and purification of the peptides were performed as previously described [31 – 33]. In this study, two PAs were synthesized: PA-S (C16-GTAGLIGQS) consisting only of a MMP-2 sensitive (GTAGLIGQ) sequence, and PA-RGDS (C16-GTAGLIGQRGDS) consisting of a MMP-2 sensitive sequence coupled to a cell adhesive ligand (RGDS) sequence. Successful PA syntheses were confirmed by MALDI-TOF mass spectrometry, and as theoretically predicted, the PA monoisotopic masses were determined to be 1368.98 (PA-RGDS) and 1040.82 (PA-S).

2.3. Self-assembly of PAs onto ePCL nanofibers

ePCL sheets were cut into 16 mm diameter scaffolds using a Humboldt boring machine (Fisher Scientific) and treated with decreasing concentrations of ethanol. A 0.1 wt. % stock solution in DI water was prepared for each PA, and their pH was adjusted to 7.4 using NaOH and HCl. 200 μl of the PA stock solutions were placed onto ePCL scaffolds. They were immediately placed on a shaker for 48 hours and then in a non-humidified 37° C incubator for 24 hours to evaporate the solvent and coat ePCL nanofibers with self-assembled PA nanofibers.

The following scaffolds were developed and used: ePCL (uncoated electrospun PCL nanofibers), ePCL-PA-S (ePCL nanofibers coated with self-assembled PA-S), and ePCL-PA-RGDS (ePCL nanofibers coated with self-assembled PA-RGDS).

2.4. Scanning electron microscope (SEM) imaging

Morphology of the ePCL nanofibers was characterized using SEM. The nanofibers were sputter coated with gold/palladium and their morphology was observed under a Philips SEM

510 at an accelerating voltage of 20 kV. SEM images were analyzed using an image analyzer (Image-proplus, Media Cybernetics Co., MD) for measurement of fiber diameters. ePCL-PA-S and ePCL-PA-RGDS scaffolds were also imaged using the same described conditions to ensure that the self-assembled PA coatings do not interfere with the ePCL nanofiber network.

2.5. Transmission electron microscope (TEM) imaging

Self-assembly of PAs into nanofibrous matrices was characterized using TEM. A 5 μl droplet of each PA stock solution was placed on a carbon coated formvar copper grid (400 mesh) and dried for 24 hours in a chemical hood to induce self-assembly. The grids were negative stained with 10 μl of 20% phosphotungstic acid (PTA) buffered to pH 7 for 30 seconds before wicking off excess. The nanofibers were observed on a Tecnai T12 microscope by FEI operated at 60 kV accelerating voltage.

Self-assembly of PAs onto ePCL nanofibers was also characterized using TEM. ePCL nanofibers were electrospun directly onto a carbon coated formvar copper grid (400 mesh). After dessicating overnight, the PAs were self-assembled onto ePCL nanofibers by placing a 3 μl droplet of the PA stock solution and subjected to the solvent evaporation process described above. The grids were then negative stained with 10 μl of 20% PTA buffered to pH 7 for 30 seconds before wicking off excess. The nanofibers were observed on a Tecnai T12 microscope operated at 120 kV accelerating voltage.

Also, to identify the long term PA coating characteristic on the hybrid nanofibers, some of the grids were incubated in PBS for 3 days and then imaged using TEM.

2.6. Examination of coating thickness on the hybrid nanofibers

TEM images of the hybrid nanofibers were analyzed using GIMP ver. 2.6 software to measure the PA nanofiber coated area. The integral of this area was calculated to determine the thickness of the PA coatings.

2.7. Evaluation of cellular behavior

Human mesenchymal stem cells (hMSCs) (Lonza, MD) were grown in 75 cm^2 cell culture flasks (Corning Glass Works, NY) with normal cell culture medium: Dulbecco's Modified Eagle's Medium (DMEM; Mediatech, VA) prepared with 10% fetal bovine serum (FBS; HyClone, UT), 1% Amphotericin B, 1% penicillin, and 1% streptomycin (Mediatech, VA). Cells were passaged using a 0.05% trypsin/EDTA (Mediatech, VA) solution when confluency reached approximately 80%. All cell cultures were maintained at standard culture conditions (37°C, 95% relative humidity, and 5% CO_2) and the culture medium was changed every 2 days.

In order to evaluate initial cell attachment and spreading, ePCL, ePCL-PA-S, and ePCL-PA-RGDS scaffolds were prepared as described above and fitted into a 48-well culture plate. The scaffold surfaces were gently flattened against the bottom of the wells to provide a uniform, flat surface for cells. Prior to cell seeding, the scaffolds were sterilized under UV for 4 hours, and then soaked in medium for 2 hours.

For the initial attachment experiment (n=4), hMSCs were seeded at a concentration of 20,000 cells/cm^2. After 1 and 4 hours, the scaffolds were washed with PBS and incubated with 0.25 % trypsin for 30 minutes at 37°C. The trypsinized solutions were collected and diluted in a 1:1 ratio with PBS and stored at -80°C. The cell attachment for each time point was measured using a fluorometric PicoGreen DNA kit (Molecular Probes Inc., OR) that quantifies the amount of double stranded DNA in cells [13, 38]. The fluorescence

absorbance from the solutions was measured using a fluorescent microplate reader (Synergy HT, BIO-TEK Instrument, VT) equipped with a 485/528 (EX/EM) filter set. A standard curve based on known concentrations of calf thymus DNA was used to determine the total amount of DNA. The cell number was calculated using a value of 7.88×10^{-6} μg of DNA/cell.

To evaluate cell spreading (n=4), hMSCs were seeded on the hybrid nanofiber scaffolds at a concentration of 20,000 cells/cm^2. After 4 hours of incubation, medium was aspirated, and each well was rinsed with PBS. Cells were then stained with calcein AM and ethidium homodimer-1 (Live–Dead Assay Kit; Molecular Probes Inc., OR). Calcein AM is converted to a green fluorescent product within live cells due to enzymatic activity of cytosolic esterases, while ethidium homodimer-1, a red fluorescent compound, accumulates in dead cells due to increased membrane permeability. Fluorescently labeled cells were observed under a Nikon fluorescent microscope. Individual cell spreading was analyzed by image processing software (NIS-elements AR 2.30). Five images from different regions were taken from each scaffold, for a total of 20 images per condition.

Additionally, after 4 hours of incubation with hMSCs (20,000 cells/cm^2), their morphology (n=4) was visualized by treatment with rhodamine-phalloidin (Molecular Probes, OR), which specifically stains actin filaments. Cells were fixed by incubation under 10% neutral buffered formalin solution for 10 minutes. The cells were then permeabilized with 0.1% Triton-X100 in PBS for 20 minutes followed by treatment with rhodamine-phalloidin for 30 minutes in a dark, humid environment. DAPI (1:40,000 in DI water) was used to counterstain the nuclei of the cells. Images were taken using a Nikon Eclipse TE2000-S fluorescent microscope.

2.8. Statistical analysis

All experiments were performed at least three independent times. All values were expressed as means ± standard deviations. One-way analysis of variance was used to check for significant differences, and Turkey multiple comparisons test was also conducted to determine significant differences between pairs. SPSS 15.0 software (SPSS Inc., IL) was used to perform statistical analysis. A $p<0.05$ was considered statistically significant.

3. Results and discussion

Tissue engineering is an emerging field that aims to restore function in previously impaired musculoskeletal and connective tissues. An ideal approach to tap into its potential is to develop a strategy that integrates both the nanofibrous interface and the bioactive cues present in native ECM. An extensively used technique to produce ECM structure mimicking scaffolds is electrospinning. While it can be used to fabricate scaffolds from both synthetic and biological polymers, such scaffolds have a variety of associated issues. Synthetic electrospun polymers are mechanically strong, but have poor hydrophilicity and bioactivity, decreasing their affinity towards cells. Although surface modification techniques, such as plasma treatment, have alleviated some issues, these treatments are harsh, and thus they compromise the nanofibrous network and mechanical properties of the electrospun scaffolds [39]. Electrospinning natural materials, such as collagen or gelatin, has drawbacks as well. In particular, there are concerns regarding structural stability and denaturing during fabrication. As noted by Rho et al., these deficiencies have made it necessary to coat electrospun collagen scaffolds with additional ECM proteins to achieve efficient cell attachment [40].

Therefore, a novel hybrid scaffold consisting of ePCL nanofibers coated with self-assembled ECM mimicking PA nanofibers has been developed (figure 1a). This scaffold has two

important components: (1) a nanofibrous ePCL network that provides the structural properties of electrospun synthetic polymers, and (2) characteristic properties of the ECM, such as bioactive cell adhesive ligands, incorporated into the PA. While the nanofibrous ePCL network provides a supportive construct for cells, the lack of cell recognition sites on its surface impedes the control of cellular behavior. This issue is remedied by the bioactive ligands presented by the self-assembled PA nanofibers coated onto the ePCL nanofibers. These cell adhesive ligands allow cell receptors to immediately recognize the scaffold surface and actively guide cell-scaffold interactions, thus creating a highly adaptable material with potential for many different applications (figure 1b).

The ePCL nanofibers were successfully fabricated with diameters between 200 nm – 700 nm, and were arranged in a random, interwoven network, as illustrated by SEM (figure 2a, 2b). Additionally, the majority of the nanofibers had diameters between 300 nm – 400 nm, which is similar to collagen fiber bundles in native ECM [41].

To overcome the lack of bioactivity of ePCL nanofibers (depicted in figure 1), ECM mimicking PAs that self-assemble into higher order structures were employed [31 – 33]. Two PAs were successfully synthesized – PA-S ($CH_3(CH_2)_{14}$CONH-GTAGLIGQ-S), and PA-RGDS ($CH_3(CH_2)_{14}$CONH-GTAGLIGQ-RGDS). Both had a hydrophobic alkyl tail coupled to a GTAGLIGQ (Gly-Thr-Ala-Gly-Leu-Ile-Gly-Gln) amino acid sequence, which is enzymatically degraded by MMP-2. PA-RGDS was functionalized with the RGDS (Arg-Gly-Asp-Ser) cell adhesive ligand, while PA-S acted as the non-adhesive control.

For this study, a solvent evaporation technique was developed to induce self-assembled coatings from the aqueous PA solutions, whereas the previous methods for achieving self-assembly were changing pH or adding divalent ions to form gel-like nanomatrices [31 – 33]. This process induces nanofiber self-assembly by increasing the concentration of the PAs to the required critical point. TEM images in figure 2c and 2d show successful PA self-assembly into nanofibers with diameters of 8 – 10 nm, and lengths of several microns, corresponding to the results of previous studies [31].

This simple solvent evaporation method was used to coat self-assembled PA nanofibers onto inert ePCL nanofibers and thus provide bioactivity. The hybrid scaffolds developed using this process have been denoted as ePCL-PA-S (ePCL nanofibers coated with self-assembled PA-S nanofibers), and ePCL-PA-RGDS (ePCL nanofibers coated with self-assembled PA-RGDS nanofibers). To ensure that the self-assembled PA nanofibers do not interfere with the nanofibrous ePCL network, it was crucial to achieve a uniform coating of PA nanofibers. SEM images of the PA coated ePCL nanofibers demonstrated that the self-assembly of the PAs specifically coated individual ePCL nanofibers and did not block the nanofibrous ePCL network (figure 3). Thus, the porous, ECM mimicking structure of the ePCL network was preserved.

Next, the self-assembly of the PAs onto individual ePCL nanofibers was characterized using TEM. As shown in figure 4, each ePCL nanofiber (central opaque regions in the images) was coated by self-assembled PA nanofibers (lighter regions on “top” and “bottom” of each ePCL nanofiber). Since imaging with TEM does not provide a depth resolution, the stage of the electron microscope was tilted in the transverse plane to demonstrate evidence of PA self-assembly all around the ePCL nanofiber. Figure 4a shows an ePCL-PA-RGDS fiber at a 0° stage tilt, while figure 4b shows the same fiber after the stage was rotated clockwise by 42°. Since both images show a layer of smaller nanofibers surrounding the larger ePCL nanofiber, it can be reasonably inferred that the PA coats the whole ePCL nanofiber. This hybrid coating characteristic was also identified in the ePCL-PA-S fiber (figure 4c and 4d).

In addition, the coating thickness was determined to be 56.12 ± 15.26 nm, which corresponds to 5-6 PA nanofibers coating each ePCL nanofiber.

To determine hybrid nanofibers' morphology at later time points, they were incubated in PBS for 3 days to simulate biological fluid conditions. As the TEM images in figure 5 demonstrate, the PAs were visible even after incubation in PBS, providing evidence that they adhere strongly to the ePCL nanofibers in the presence of a fluid medium. Figure 5 also shows that these hybrid nanofibers had the same characteristics as the ones in figure 4, indicating that soaking in medium has no adverse effects on the coating. The vital results in figures 3, 4, and 5 confirm that individual ePCL nanofibers can be coated by several self-assembled PA nanofibers to produce hybrid, nanofibrous scaffolds without causing any structural deviations, and thus suggest a new and important method for functionalizing ePCL nanofibers.

Bioactivity in the newly developed hybrid scaffolds is provided explicitly by the outer peptide region of the PA molecules. The RGDS ligand was chosen as the bioactive signal, because it is found in various ECM molecules and its integrin-ligand mechanism has been well studied [34, 35]. The inclusion of the RGDS ligand gives the PA molecules a conical shape, which results in the cylindrical micelle shape after self-assembly, as the most energetically favorably conformation is with the hydrophilic peptide regions on the outside and the hydrophobic tails shielded within the core of the nanofibers [31, 42]. This conformation enables the cells to recognize, and interact with the functionalized peptide domains.

To evaluate the bioactivity conferred by the PAs to the ePCL nanofibers, initial attachment, spreading, and cytoskeletal morphologies of hMSCs on ePCL, ePCL-PA-S, and ePCL-PA-RGDS were studied. The initial cell attachment study demonstrated significantly greater hMSC attachment at both 1 and 4 hours on ePCL-PA-RGDS as compared to either ePCL or ePCL-PA-S ($p<0.05$) (figure 6). Furthermore, cell attachment on ePCL-PA-S was significantly greater after 4 hours than on ePCL ($p<0.01$). Attachment on ePCL-PA-RGDS increased ~30%, from 15454.76 ± 2567.34 cells/cm^2 at 1 hour to 19927.06 ± 1747.42 cells/cm^2 after 4 hours. Cell attachment on ePCL-PA-S increased by ~20% between the two timepoints, rising from 11296.31 ± 810.35 cells/cm^2 to 13571.69 ± 784.61 cells/cm^2. However, attachment on ePCL remained essentially constant with values of 11453.23 ± 543.60 cells/cm^2 at 1 hour and 10197.85 ± 543.60 cells/cm^2 after 4 hours. Overall, these results clearly show that hMSCs immediately recognize the inscribed RGDS cell adhesive ligand in ePCL-PA-RGDS, and attach in preferentially greater numbers on this scaffold.

hMSC spreading and morphology were characterized using a Live/Dead assay and rhodamine – phalloidin staining, and representative images have been shown in figure 7. It is evident that the extent of spreading increases across the three different scaffolds. Cells on unmodified ePCL exhibited rounded morphologies with very few cytoskeletal extensions, and only a few cells appeared to be starting to spread on ePCL-PA-S. This is in striking contrast to the cells on ePCL-PA-RGDS, which adopted well spread morphologies. The percentage of spreading cells was also quantified by image analysis and shown in figure 8. The percentage of spreading cells increased significantly from 17.00 ± 2.84 % on ePCL to 26.56 ± 5.48 % on ePCL-PA-S ($p<0.05$) to 41.60 ± 2.04 % on ePCL-PA-RGDS ($p<0.01$). The rhodamine – phalloidin staining also showed a similar trend for F-actin stress fiber formation: hMSCs on ePCL and ePCL-PA-S were small and had limited stress fiber formation, whereas cells on ePCL-PA-RGDS were larger and showed much greater stress fiber formation. These results demonstrate that cells favor the bioactive substrate presented by ePCL-PA-RGDS.

The central concepts highlighted by this study are that (1) a nanofibrous ePCL scaffold used by itself will never fully realize its potential in tissue engineering, and (2) the improvement in cellular behavior was directly correlated to the extent of modification of the ePCL nanofibers. ePCL showed lowest amounts of attachment and spreading, followed by ePCL-PA-S, and then ePCL-PA-RGDS, which demonstrated the best attachment and spreading. One possible reason for the increase in the cellular performance for ePCL-PA-S is the improvement in the hydrophilicity of the scaffolds due to the presence of amine and carboxyl groups in PA-S. Furthermore, the large increases in attachment and spreading due to the RGDS ligand leads to reasonable inferences that addition of cell adhesive ligands greatly improves the bioactivity of ePCL scaffolds, and that they are effective mediators of cellular behaviors.

The combination of self-assembled PAs coated onto ePCL nanofibers has numerous advantages. This hybrid system can be easily tailored for individual biological applications by simply changing the cell-adhesive ligand sequence in the PAs. Future plans aim to take advantage of this versatility and develop scaffolds for specific cells and tissues. For example, the amino acid sequences VAPG (Val-Ala-Pro-Gly), isolated from elastin, and YIGSR (Tyr-Ile-Gly-Ser-Arg), isolated from laminin, have been shown to support the adhesion of smooth muscle cells and endothelial cells respectively, and their incorporation into the hybrid scaffolds has great promise for vascular tissue regeneration [43 – 45]. Similarly, a number of other tissue-specific ligand sequences have been identified and could potentially be used for regenerating a variety of tissues. Additionally, the PAs can be coated onto different electrospun polymers to meet the specific mechanical needs of the tissue under consideration [46]. A unique feature of this hybrid system is that along with presenting a nanofibrous morphology of an electrospun polymer, the inscribed cell adhesive ligands in the PAs provide all the necessary stimuli to enable stem cell differentiation or for maintaining the differentiated phenotype of cell, eliminating any need for media supplements that would otherwise be required. These distinctive characteristics make this novel method of mimicking ECM structure and function by self-assembling PAs onto electrospun fibers an exciting development in tissue regeneration.

4. Conclusions

Electrospinning is an extensively used process to fabricate fibrous scaffolds mimicking the topography of the ECM, but the bioactivity of such scaffolds is limited. Therefore, this study demonstrated the development of a hybrid, bioactive scaffold by coating inert ePCL nanofibers with self-assembled, ECM mimicking PA nanofibers. Overall, this novel strategy provides a new solution to overcome the current drawback of electrospun scaffolds by combining the characteristics of the ePCL nanofibers and self-assembled PA nanofibers to create an ECM mimicking environment. This has great promise across many different types of electrospun scaffolds and can be used for various biomedical applications.

Acknowledgments

The authors acknowledge the efforts of Dr. Robin Foley for SEM imaging and Melissa Chimento and the High Resolution Imaging Facility for TEM imaging. We express thanks to the Mass Spectrometry/Proteomics Shared Facility for analysis of the molecular weights of all PAs. We also appreciate the help of all students, especially Himani Deshpande, in Dr. Derrick Dean's lab, with the electrospinning apparatus. This work has been supported by the Wallace H. Coulter Foundation (H.W.J), the 2007 Intramural Pilot Grant from the BioMatrix Engineering and Regenerative Medicine Center at UAB (H.W.J), T32EB004312 from the NIBIB (J.A), and the Caroline P. Ireland Research Scholarship (M.K and A.A).

References

1. Hubbell JA. Materials as morphogenetic guides in tissue engineering. Curr Opin Biotechnol. 2003; 14:551–58. [PubMed: 14580588]
2. Kleinman HK, Philp D, Hoffman MP. Role of the extracellular matrix in morphogenesis. Curr Opin Biotechnol. 2003; 14:526–32. [PubMed: 14580584]
3. Streuli C. Extracellular matrix remodelling and cellular differentiation. Curr Opin Cell Biol. 1999; 11:634–40. [PubMed: 10508658]
4. Daley WP, Peters SB, Larsen M. Extracellular matrix dynamics in development and regenerative medicine. J Cell Sci. 2008; 121:255–64. [PubMed: 18216330]
5. Li WJ, Jiang YJ, Tuan RS. Chondrocyte phenotype in engineered fibrous matrix is regulated by fiber size. Tissue Eng. 2006; 12:1775–85. [PubMed: 16889508]
6. Yang S, Leong K, Du Z, Chua C. The Design of Scaffolds for Use in Tissue Engineering. Part I. Traditional Factors. Tissue Eng. 2001; 7:679–89. [PubMed: 11749726]
7. Li WJ, Danielson KG, Alexander PG, Tuan RS. Biological response of chondrocytes cultured in three-dimensional nanofibrous poly(e-caprolactone) scaffolds. J Biomed Mater Res A. 2003; 67:1105–14. [PubMed: 14624495]
8. Choi JS, Lee SJ, Christ GJ, Atala A, Yoo JJ. The influence of electrospun aligned poly(epsilon-caprolactone)/collagen nanofiber meshes on the formation of self-aligned skeletal muscle myotubes. Biomaterials. 2008; 29:2899–906. [PubMed: 18400295]
9. Venugopal J, Ma LL, Yong T, Ramakrishna S. In vitro study of smooth muscle cells on polycaprolactone and collagen nanofibrous matrices. Cell Biol Int. 2005; 29:861–7. [PubMed: 16153863]
10. Ma Z, He W, Yong T, Ramakrishna S. Grafting of gelatin on electrospun poly(caprolactone) nanofibers to improve endothelial cell spreading and proliferation and to control cell Orientation. Tissue Eng. 2005; 11:1149–58. [PubMed: 16144451]
11. Zhang YZ, Venugopal J, Huang ZM, Lim CT, Ramakrishna S. Characterization of the surface biocompatibility of the electrospun PCL-Collagen nanofibers using fibroblasts. Biomacromolecules. 2005; 6:2583–89. [PubMed: 16153095]
12. Yoshimoto H, Shin YM, Terai H, Vacanti JP. A biodegradable nanofiber scaffold by electrospinning and its potential for bone tissue engineering. Biomaterials. 2003; 24:2077–82. [PubMed: 12628828]
13. Li WJ, Tuli R, Okafor C, Derfoul A, Danielson KG, Hall DJ, Tuan RS. A three-dimensional nanofibrous scaffold for cartilage tissue engineering using human mesenchymal stem cells. Biomaterials. 2005; 26:599–609. [PubMed: 15282138]
14. Venugopal J, Low S, Choon AT, Kumar AB, Ramakrishna S. Electrospun – modified nanofibrous scaffolds for the mineralization of osteoblast cells. J Biomed Mater Res A. 2008; 65:408–17. [PubMed: 17701970]
15. Nisbet DR, Yu LMY, Zahir T, Forsythe JS, Shoichet MS. Characterization of neural stem cells on electrospun poly(ε-caprolactone) submicron scaffolds: evaluating their potential in neural tissue engineering. J Biomater Sci Polym Ed. 2008; 19:623–34. [PubMed: 18419941]
16. Kim CH, Khil MS, Kim HY, Lee HU, Jahng KY. An improved hydrophilicity via electrospinning for enhanced cell attachment and proliferation. J Biomed Mater Res B. 2006; 78:283–90.
17. Jia J, Duan YY, Yu J, Lu JW. Preparation and immobilization of soluble eggshell membrane protein on the electrospun nanofibers to enhance cell adhesion and growth. J Biomed Mater Res A. 2008; 86:364–73. [PubMed: 17969029]
18. Matthews JA, Wnek GE, Simpson DG, Bowlin GL. Electrospinning of collagen nanofibers. Biomacromolecules. 2002; 3:232–8. [PubMed: 11888306]
19. Buttafoco L, Kolkman NG, Engbers-Buijtenhuijs P, Poot AA, Dijkstra PJ, Vermes I, Feijen J. Electrospinning of collagen and elastin for tissue engineering applications. Biomaterials. 2006; 27:724–34. [PubMed: 16111744]
20. Li M, Mondrinos MJ, Gandhi MR, Ko FK, Weiss AS, Lelkes PI. Electrospun protein fibers as matrices for tissue engineering. Biomaterials. 2005; 26:5999–6008. [PubMed: 15894371]

21. Zhang Y, Ouyang H, Lim CT, Ramakrishna S, Huang ZM. Electrospinning of gelatin fibers and gelatin/PCL composite fibrous scaffolds. J Biomed Mater Res Appl Biomater B. 2005; 72:156–65.
22. Schnell E, Klinkhammer K, Balzer S, Brook G, Klee D, Dalton P, Mey J. Guidance of glial cell migration and axonal growth on electrospun nanofibers of poly-epsilon-caprolactone and a collagen/poly-epsilon-caprolactone blend. Biomaterials. 2007; 28:3012–25. [PubMed: 17408736]
23. Heydarkhan-Hagvall S, Schenke-Layland K, Dhanasopon AP, Rofail F, Smith H, Wu BM, Shemin R, Beygui RE, MacLellan WR. Three-dimensional electrospun ECM-based hybrid scaffolds for cardiovascular tissue engineering. Biomaterials. 2008; 29:2907–14. [PubMed: 18403012]
24. Ghasemi-Mobarakeh L, Prabhakaran MP, Morshed M, Nasr-Esfahani MH, Ramakrishna S. Electrospun poly(epsilon-caprolactone)/gelatin nanofibrous scaffolds for nerve tissue engineering. Biomaterials. 2008; 29:4532–39. [PubMed: 18757094]
25. Zhao P, Jiang H, Pan H, Zhu K, Chen W. Biodegradable fibrous scaffolds composed of gelatin coated poly(epsilon-caprolactone) prepared by coaxial electrospinning. J Biomed Mater Res A. 2007; 83:372–82. [PubMed: 17450578]
26. Thomas V, Jagani S, Johnson K, Jose MV, Dean DR, Vohra YK, Nyairo E. Electrospun bioactive nanocomposite scaffolds of polycaprolactone and nanohydroxyapatite for bone tissue engineering. J Nanosci Nanotechnol. 2006; 6:487–93. [PubMed: 16573049]
27. Prabhakaran MP, Venugopal JR, Chyan TT, Hai LB, Chan CK, Lim AY, Ramakrishna S. Electrospun biocomposite nanofibrous scaffolds for neural tissue engineering. Tissue Eng A. 2008; 14:1787–97.
28. Venugopal J, Ramakrishna S. Biocompatible nanofiber matrices for the engineering of a dermal substitute for skin regeneration. Tissue Eng. 2005; 11:847–54. [PubMed: 15998224]
29. Li X, Xie J, Yuan X, Xia Y. Coating Electrospun Poly(epsilon-caprolactone) Fibers with Gelatin and Calcium Phosphate and Their Use as Biomimetic Scaffolds for Bone Tissue Engineering. Langmuir. 2008; 24:14145–50. [PubMed: 19053657]
30. Oyane A, Uchida M, Yokoyama Y, Choong C, Triffitt J, Ito A. Simple surface modification of poly(epsilon-caprolactone) to induce its apatite-forming ability. J Biomed Mater Res A. 2005; 75:138–45. [PubMed: 16044403]
31. Jun HW, Yuwono V, Paramonov SE, Hartgerink JD. Enzyme-mediated degradation of peptide-amphiphile nanofiber networks. Adv Mater. 2005; 17:2612–17.
32. Paramonov SE, Jun HW, Hartgerink JD. Self-assembly of peptide-amphiphile nanofibers: the roles of hydrogen bonding and amphiphilic packing. J Am Chem Soc. 2006; 128:7291–98. [PubMed: 16734483]
33. Hartgerink JD, Beniash E, Stupp SI. Self-assembly and mineralization of peptide-amphiphile nanofibers. Science. 2001; 294:1684–88. [PubMed: 11721046]
34. Pierschbacher MD, Ruoslahti E. Cell attachment activity of fibronectin can be duplicated by small synthetic fragments of the molecule. Nature. 1984; 309:30–3. [PubMed: 6325925]
35. Hersel U, Dahmen C, Kessler H. RGD modified polymers: biomaterials for stimulated cell adhesion and beyond. Biomaterials. 2003; 24:4385–15. [PubMed: 12922151]
36. Bryant SJ, Anseth KS. Hydrogel properties influence ECM production by chondrocytes photoencapsulated in poly(ethylene glycol) hydrogels. J Biomed Mater Res. 2002; 59:63–72. [PubMed: 11745538]
37. Nagase H, Fields GB. Human matrix metalloproteinase specificity studies using collagen sequence-based synthetic peptides. Biopolymers. 1996; 40:399–416. [PubMed: 8765610]
38. Pham QP, Sharma U, Mikos AG. Electrospun poly(epsilon-caprolactone) microfiber and multilayer nanofiber/microfiber scaffolds: characterization of scaffolds and measurement of cellular infiltration. Biomacromolecules. 2006; 7:2726–805.
39. Ma Z, Kotaki M, Yong T, He W, Ramakrishna S. Surface engineering of electrospun polyethylene terephthalate (PET) nanofibers towards development of a new material for blood vessel engineering. Biomaterials. 2005; 26:2527–36. [PubMed: 15585255]
40. Rho KS, Jeong L, Lee G, Seo BM, Park YJ, Hong SD, Roh S, Cho JJ, Park WH, Min BM. Electrospinning of collagen nanofibers: effects on the behavior of normal human keratinocytes and early-stage wound healing. Biomaterials. 2006; 27:1452–61. [PubMed: 16143390]

41. Elsdale T, Bard J. Collagen substrata for studies on cell behavior. J Cell Biol. 1972; 54:626–37. [PubMed: 4339818]

42. Hartgerink JD, Beniash E, Stupp SI. Peptide-amphiphile nanofibers: a versatile scaffold for the preparation of self-assembling materials. Proc Natl Acad Sci USA. 2002; 99:5133–38. [PubMed: 11929981]

43. Mann BK, West JL. Cell adhesion peptides alter smooth muscle cell adhesion, proliferation, migration, and matrix protein synthesis on modified surfaces and in polymer scaffolds. J Biomed Mater Res. 2002; 60:86–93. [PubMed: 11835163]

44. Gobin AS, West JL. Val-Ala-Pro-Gly, an elastin derived non-integrin ligand: Smooth muscle cell adhesion and specificity. J Biomed Mater Res A. 2003; 67:255–59. [PubMed: 14517884]

45. Jun HW, West JL. Development of a YIGSR peptide modified polyurethaneurea to enhance endothelialization. J Biomater Sci Polym Ed. 2004; 15:73–94. [PubMed: 15027844]

46. Li WJ, Cooper JA, Mauck RL, Tuan RS. Fabrication and characterization of six electrospun poly(α-hydroxy ester)- based fibrous scaffolds for tissue engineering applications. Acta Biomaterilia. 2006; 2:377–85.

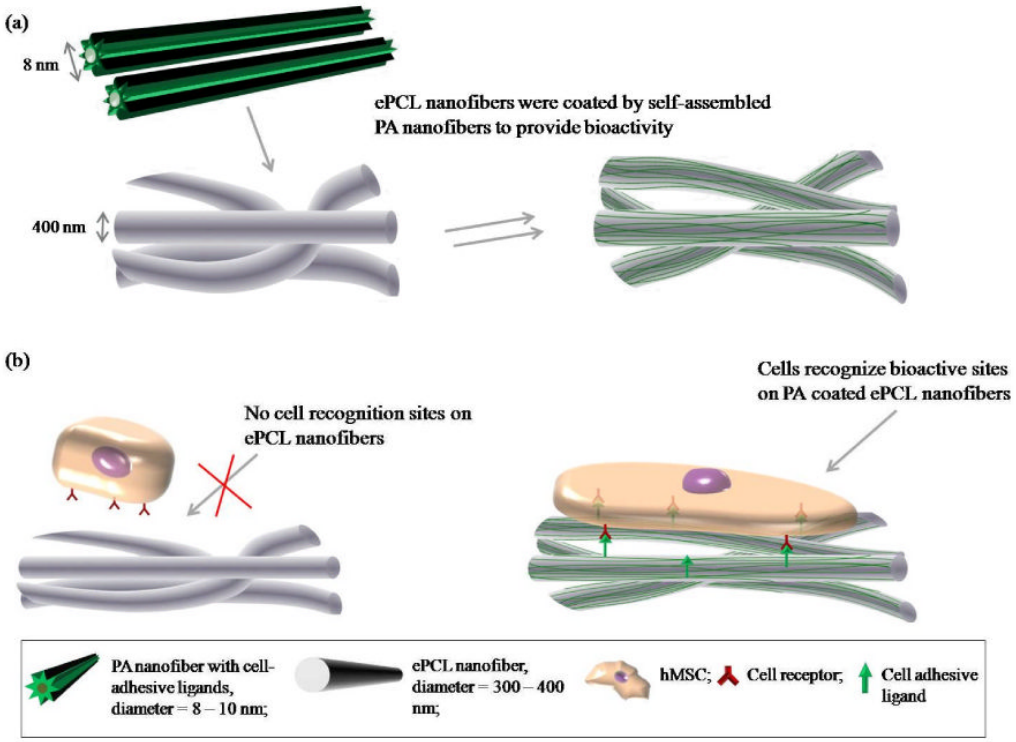

Figure 1.

(a) Fabrication method for the hybrid nanofibers: inert ePCL nanofibers were coated by self-assembled ECM mimicking PA nanofibers to provide bioactivity. (b) Rationale for the hybrid nanofibers: the lack of cell recognition sites on ePCL nanofibers limits cell-scaffold interactions. In contrast, bioactive cell adhesive ligands on the PA coated ePCL nanofibers can control cellular behaviors.

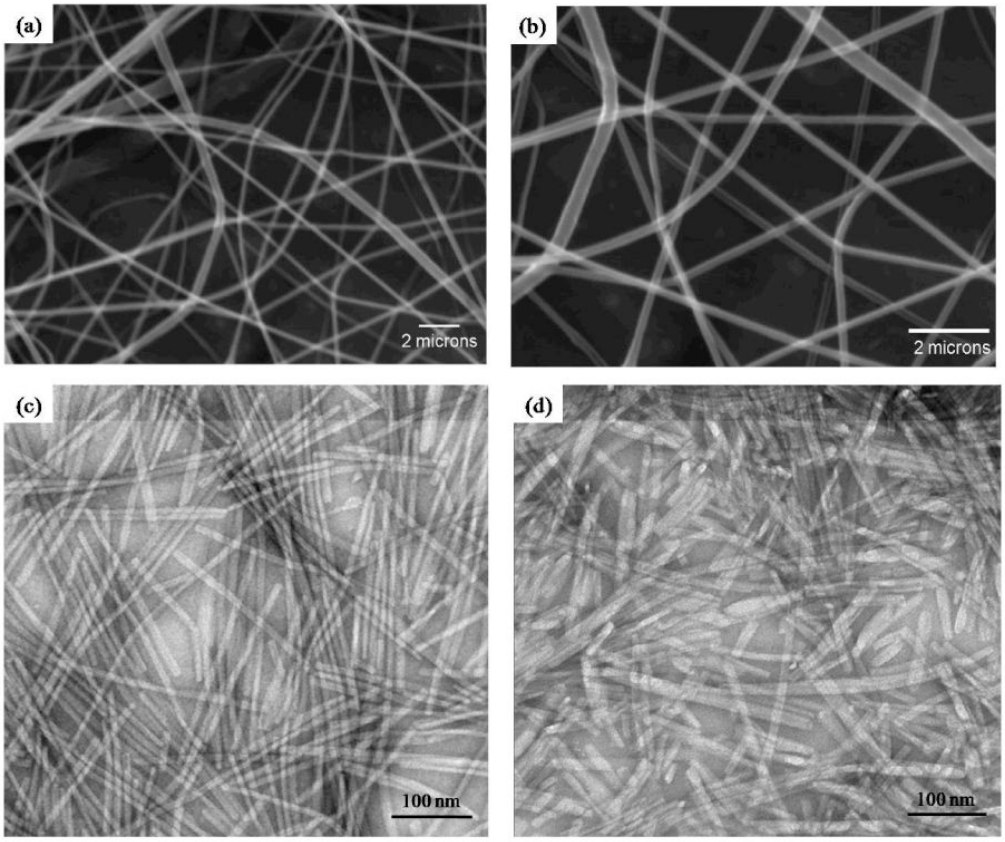

Figure 2.
SEM images show ePCL nanofibers fabricated into an interwoven, porous network at (a) 7400× and (b) 14800×. TEM images show successful PA self-assembly into nanofibers of (c) PA-RGDS and (d) PA-S.

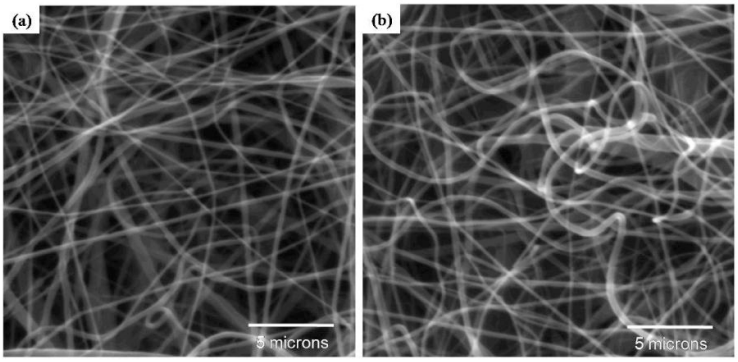

Figure 3.
SEM images of (a) ePCL-PA-RGDS and (b) ePCL-PA-S show successful fabrication of the hybrid scaffolds, and demonstrate that the PA nanofibers did not interfere with the nanofibrous ePCL network.

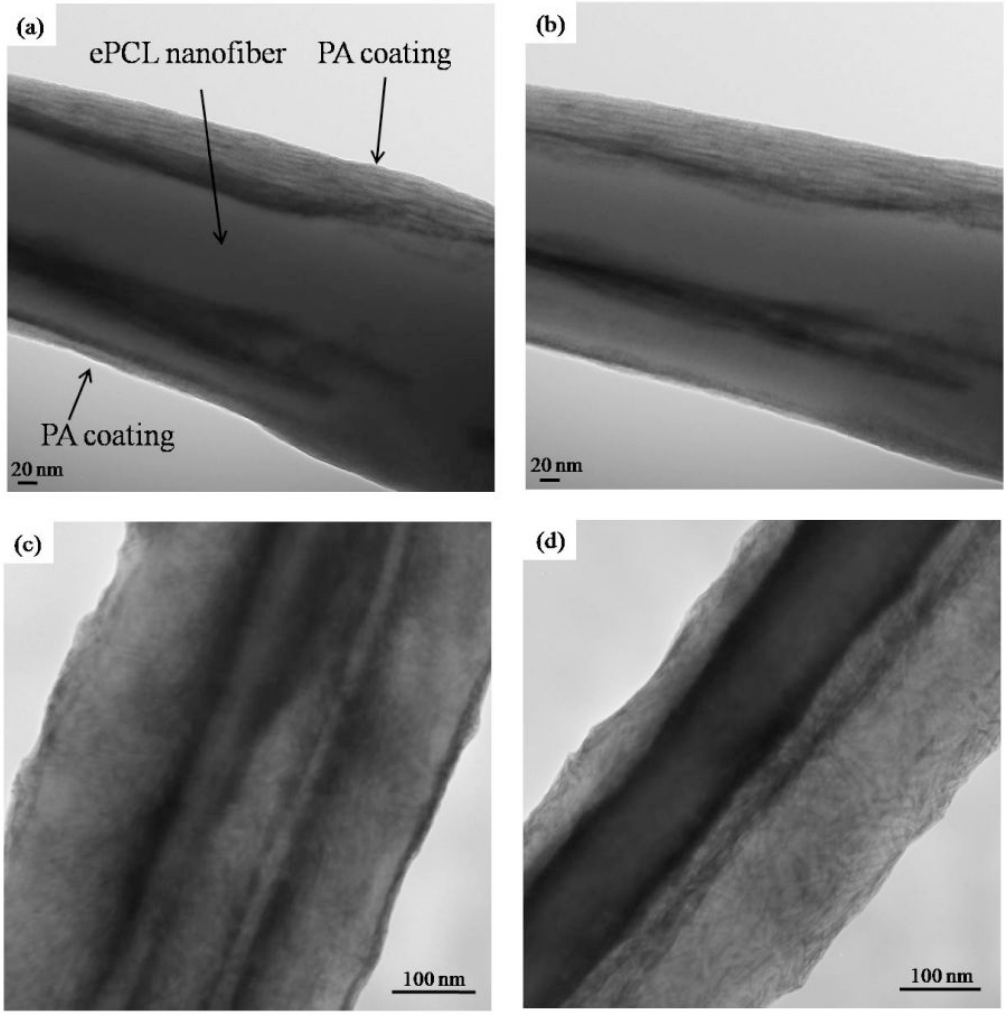

Figure 4.
TEM images show successful self-assembly of PAs onto ePCL nanofibers to create the hybrid nanofibers. (a) ePCL-PA-RGDS at 0° tilt, (b) ePCL-PA-RGDS at 42° tilt, (c) ePCL-PA-S at 0° tilt, (d) ePCL-PA-S at 46° tilt. Presence of PA nanofibers on both tilted and un-tilted images indicates that the PAs coated all around each ePCL nanfiber.

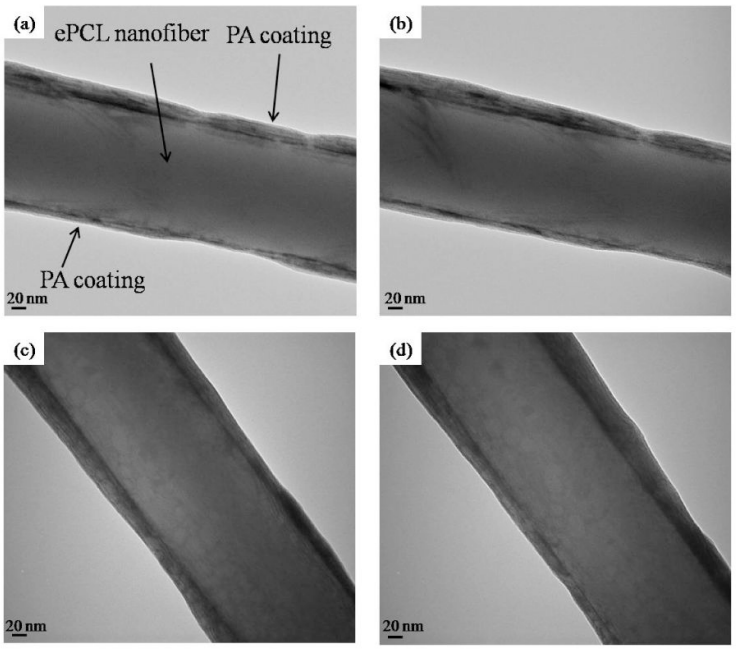

Figure 5.
TEM images of hybrid nanofibers after soaking in PBS for 3 days show similar characteristics as those not soaked in PBS, and demonstrate that PA nanofibers adhered strongly to ePCL nanofibers even in a fluid medium. (a) untilted ePCL-PA-RGDS, (b) tilted ePCL-PA-RGDS, (c) untilted ePCL-PA-S, and (d) tilted ePCL-PA-S.

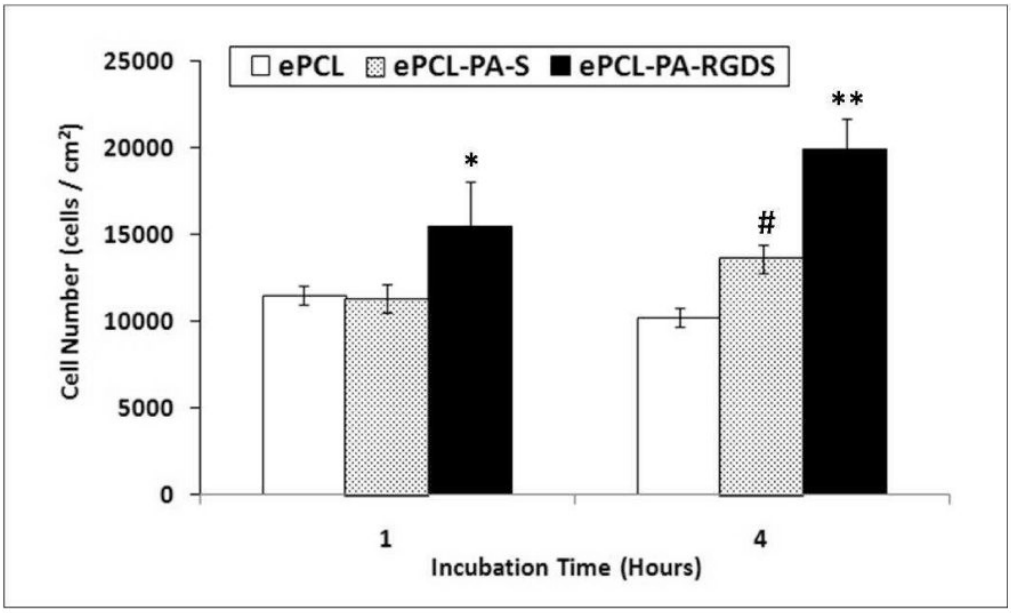

Figure 6.

Initial attachment of hMSCs shows that at both timepoints, significantly higher numbers of cells attached on ePCL-PA-RGDS compared to ePCL and ePCL-PA-S (*: $p<0.05$, **: $p<0.01$). After 4 hours, cell attachment was significantly higher on ePCL-PA-S compared to ePCL (#: $p<0.01$). Error bars represent means ± standard deviation. n = 4.

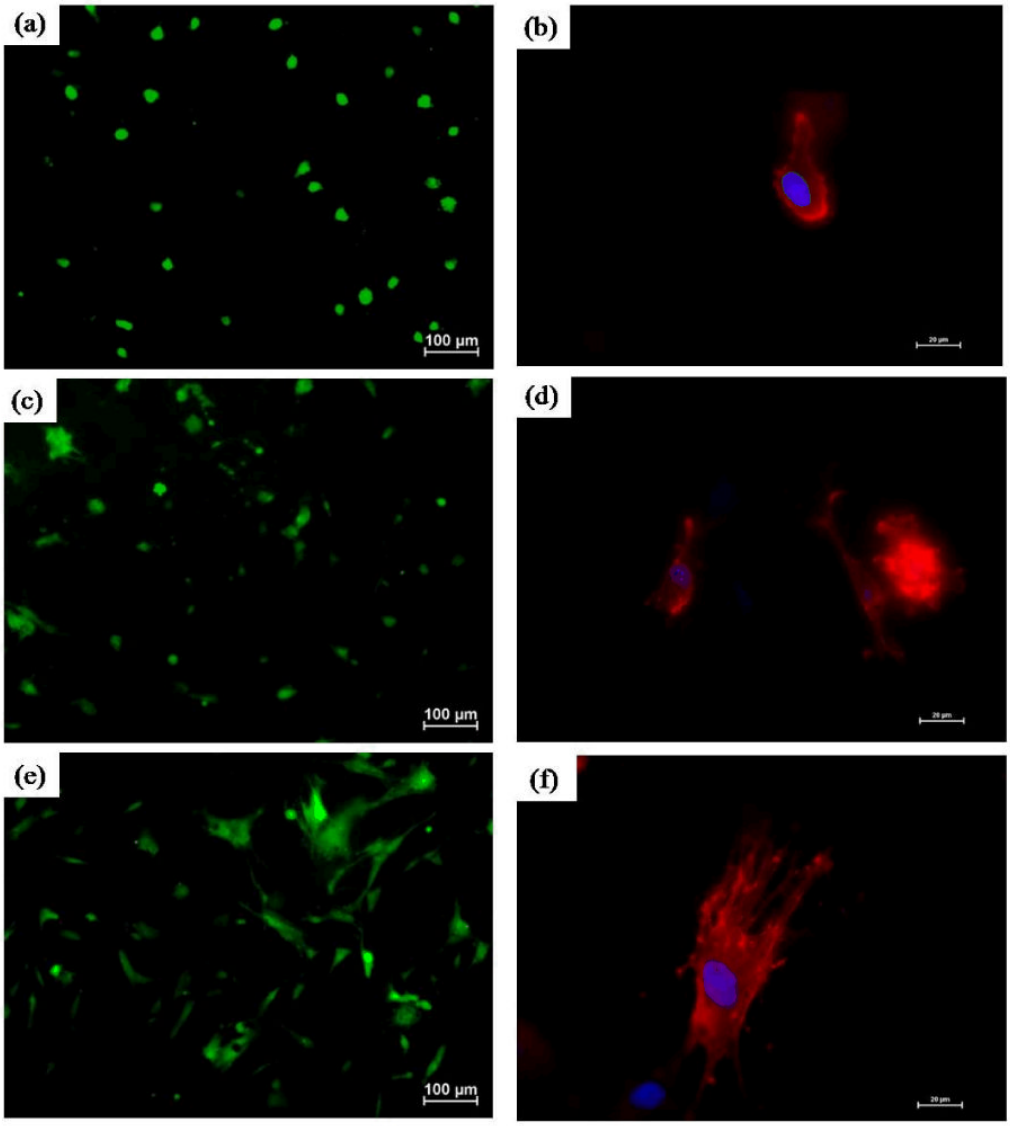

Figure 7.

Representative images of hMSC spreading using Live/Dead assay on (a) ePCL (c) ePCL-PA-S, and (e) ePCL-PA-RGDS. Magnification = 10×, scale bars = 100 μm. Representative images of hMSC morphologies using rhodamine-phalloidin staining on (b) ePCL, (d) ePCL-PA-S, and (f) ePCL-PA-RGDS. Magnification = 40×, scale bars = 20 μm. These images clearly show that cells were more spread and had greater F-actin fiber formation on ePCL-PA-RGDS than on ePCL or ePCL-PA-S.

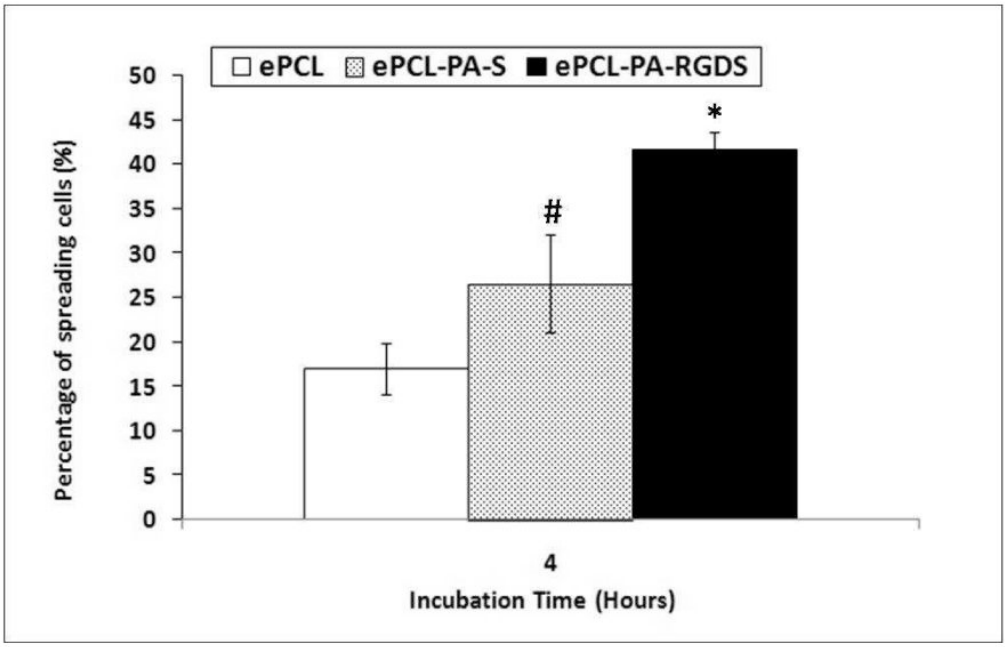

Figure 8.

Cell spreading plotted as a percentage of spread cells compared to total cells 4 hours post seeding shows that a significantly higher percentage of cells adopted spread morphologies on ePCL-PA-RGDS compared to ePCL and ePCL-PA-S (*: $p<0.01$). Cells on ePCL-PA-S also spread in significantly higher percentages compared to ePCL (#: $p<0.05$). Error bars represent means ± standard deviation. n = 4.